J Mol Evol (2002) 55:161–179
DOI: 10.1007/s00239-002-2313-5

JOURNAL OF MOLECULAR EVOLUTION

Nuclear and Nucleomorph SSU rDNA Phylogeny in the Cryptophyta and the Evolution of Cryptophyte Diversity

Kerstin Hoef-Emden, Birger Marin, Michael Melkonian

Universität zu Köln, Botanisches Institut, Lehrstuhl I, Gyrhofstr. 15, 50931 Köln, Germany

Received: 9 August 2001 / Accepted: 25 January 2002

Abstract. The plastid-bearing members of the Cryptophyta contain two functional eukaryotic genomes of different phylogenetic origin, residing in the nucleus and in the nucleomorph, respectively. These widespread and diverse protists thus offer a unique opportunity to study the coevolution of two different eukaryotic genomes within one group of organisms. In this study, the SSU rRNA genes of both genomes were PCR-amplified with specific primers and phylogenetic analyses were performed on different data sets using different evolutionary models. The results show that the composition of the principal clades obtained from the phylogenetic analyses of both genes was largely congruent, but striking differences in evolutionary rates were observed. These affected the topologies of the nuclear and nucleomorph phylogenies differently, resulting in long-branch attraction artifacts when simple evolutionary models were applied. Deletion of long-branch taxa stabilized the internal branching order in both phylogenies and resulted in a completely resolved topology in the nucleomorph phylogeny. A comparison of the tree topologies derived from SSU rDNA sequences with characters previously used in cryptophyte systematics revealed that the biliprotein type was congruent, but the type of inner periplast component incongruent, with the molecular trees. The latter is indicative of a hidden cellular dimorphism (cells with two periplast types present in a single clonal strain) of presumably widespread occurrence throughout cryptophyte diversity, which, in consequence, has far-reaching implications for cryptophyte systematics as it is practiced today.

Key words: Cryptophyta — Cryptomonads — Nucleomorph — Coevolution — SSU rRNA — Phylogeny — Dimorphism — *Cryptomonas* — Biliproteins — Periplast — *Campylomonas*

Introduction

Colorful biflagellate unicells of the division Cryptophyta are found in marine, brackish, and freshwater habitats and have evolved an astounding diversity, resulting in descriptions of more than 20 genera and approximately 200 species (e.g., Butcher 1967; Huber-Pestalozzi 1967; Clay et al. 1999). Except for the phagotrophic genus *Goniomonas* (Mignot 1965; McFadden et al. 1994b), the cryptophytes contain a plastid which presumably derived from an endocytobiosis of a photoautotrophic eukaryotic cell and was transformed to a complex plastid [surrounded by more than two envelope membranes (Sitte 1993)]. Whereas in most other organisms with complex plastids, the cytoplasm and the nucleus of the eukaryotic symbiont were lost completely, in the Cryptophyta some remnants of a eukaryotic cell can still be found: a periplastidial space located between the two outer and the two inner envelope membranes harbors a DNA-containing membrane-bound organelle termed nucleomorph and, in addition, 80S ribosomes and starch grains (Greenwood 1974; McFadden et al. 1994a). The reduced nucleomorph represents a second eukaryotic genome in addition to the nucleus of the host cell

Correspondence to: Kerstin Hoef-Emden; *email:* kerstin.hoef-emden@uni-koeln.de

(Douglas et al. 2001). Phylogenetic analyses, especially those comparing nuclear and nucleomorph SSU rRNA genes, showed that the eukaryotic genomes of the cryptophyte host cell and of the complex plastid are of different origin (Douglas et al. 1991; Cavalier-Smith et al. 1996). The origin of the host cell cannot be resolved unambiguously: in SSU rDNA trees the cryptophyte nuclear sequences cluster with low bootstrap support with the cyanelle-bearing glaucocystophytes (Bhattacharya et al. 1995; Van de Peer et al. 2000), but not necessarily in phylogenetic trees constructed using other genes, e.g., tubulin (Keeling et al. 1999), whereas it is generally accepted that the ancestor of the complex cryptophyte plastid was a rhodophyte alga (Douglas and Penny 1999). Each photoautotrophic cryptophyte clone is supplied with a single biliprotein as an accessory pigment not organized in phycobilisomes but located in the thylakoid lumen (Gantt et al. 1971; Hill and Rowan 1989; Ludwig and Gibbs 1989). Immunological and phylogenetic analyses of the biliproteins show that all biliprotein types found in the different cryptophyte genera, irrespective of their red or blue color, are derived from rhodophyte phycoerythrins (MacColl et al. 1976; Apt et al. 1995).

Today, the systematics of the cryptophytes is based on ultrastructural features unique to this group of organisms, such as the structure of the periplast [a sandwich-like cell boundary made up of an inner and an outer proteinaceous layer with the plasma membrane embedded in between (Brett et al. 1994)], the position of the nucleomorph (Gillott and Gibbs 1980), the flagellar root system (e.g., Roberts et al. 1981; Gillott and Gibbs 1983), the furrow/gullet system [a cell invagination of tubular to furrow-like appearance lined with explosive organelles, the ejectisomes (Morrall and Greenwood 1980; Kugrens et al. 1986)], and, in addition, the type of biliprotein (Hill and Rowan 1989).

The first phylogenetic analysis of cryptophyte nuclear and nucleomorph SSU rDNA sequences (Cavalier-Smith et al. 1996) contained only two taxa with phycocyanins and few taxa with phycoerythrins (representing only one of three known phycoerythrin types); this study apparently revealed a basal dichotomy between blue (phycocyanin-containing) and red (phycoerythrin-containing) cryptophytes. In contrast, a more recent study using nuclear SSU rRNA sequences of several taxa representing all known types of phycoerythrin (three types) and three of four known types of phycocyanin revealed that the characters blue and red pigmentation do not correspond with a basal dichotomy in cryptophyte evolution; instead, phycocyanins and phycoerythrins can occur within a single clade, i.e., the genus *Hemiselmis* (Marin et al. 1998).

Thus, this study focuses on a comparative phylogenetic analysis of nucleomorph and nuclear SSU rDNA sequences in the cryptophytes. Taxa were sampled to represent all known biliprotein types and different combinations of morphological characters. Both nuclear and nucleomorph SSU rDNA sequences of each new taxon were determined and missing nucleomorph sequences of other taxa were added if possible. In total 21 new nucleomorph and 10 new nuclear SSU rDNA sequences were included in the analyses. Finally, the congruence or incongruence of the tree topologies with the biliprotein types and other characters used in cryptophyte systematics is evaluated.

Materials and Methods

Algal Cultures

In Table 1, the strains examined in this study are listed with the accession numbers (EMBL) of their corresponding SSU rDNA sequences. Freshwater strains were cultivated in WARIS-H, and marine strains were grown in ESM or ASP-H [(McFadden and Melkonian 1986; Starr and Zeikus 1993); ASP-H was modified by using the trace metals solution of the L1 medium (Guillard and Hargraves 1993)]. Strains were grown at 15 ± 2°C under a light/dark cycle of 14/10 h (light intensity, between 15 and 30 μmol photons m^{-2} s^{-1}; Osram L18 W/25 Universal Weiβ). Cultures not available in public culture collections can be obtained from the authors upon request.

DNA Isolation, PCR, and Sequencing

Total genomic DNA was isolated using a CTAB protocol (Doyle and Doyle 1990; modified according to Surek et al. 1994). To amplify nucleomorph or nuclear SSU rDNA by the polymerase chain reaction (PCR) (Saiki et al. 1988) universal eukaryotic SSU rDNA primers were combined with nucleus- or nucleomorph-specific primers [cycling conditions: predenaturation for 3 min at 95°C, followed by 30 cycles of 1 min at 95°C, 2 min at 60 or 65°C, 3 min at 68°C; Primus 96 Plus thermocycler (MWG Biotech); for primer sequences and primer combinations see Table 2; for position of PCR primers, see Fig. 1]. In primer combinations 1 to 3 a biotinylated version of the nucleomorph-specific primer published by Cavalier-Smith et al. (1996) (labeled CrNM1F in this study) was used (Table 2). Since this primer amplified nuclear SSU rDNA in some taxa (e.g., strain M0739; Table 1), new nucleomorph-specific primers were designed as follows. We sequenced and aligned approximately the first 700 bases of the nuclear and nucleomorph LSU rDNA region included in primary PCR products of the SSU rDNA [nucleomorph-specific primer combination 2; nucleus-specific primer combination 9 (Table 2); nucleomorph sequences of strains M1312, M0420, and SCCAP K-0434, plus CCMP 327 (accession No. Y11510); nuclear sequences of strains M1318, M0420, and SCCAP K-0434]. The consensi of the partial nuclear and nucleomorph LSU rDNA sequences were then used to construct the reverse primers NMITS044R and NMITS055R, located in the nucleomorph LSU rDNA region. NMITS044R turned out to be the best nucleomorph-specific primer (Table 1).

Prior to sequencing, PCR products were purified using the Dynabeads M-280 system (Dynal) (Hultman et al. 1991). Sequencing reactions were performed using the SequiTherm Excel II Long Read Sequencing Kit-LC (Epicentre Technologies) and 5′-labeled primers (Table 2) [cycling conditions: predenaturation for 2 min at 95°C, followed by 30 cycles of 30 s at 94°C, 30 s at 40°C, 1 min at 70°C; Primus 96 Plus thermocycler (MWG Biotech)]. Complete SSU rDNA sequences, except for small single-stranded regions at the 5′ and 3′ ends,

Table 1. Strains used for sequencing, including origin, culture medium (see Materials and Methods), accession numbers of SSU rDNA sequences, and numbers of primer combination used to amplify the nucleomorph and/or nuclear SSU rDNA sequences[a]

Taxon	Strain	Culture medium	Accession number		Primer comb. (see Table 2), num/nuc
			Num	Nuc[b]	
Campylomonas reflexa	CCMP 152	WARIS-H	AJ420675	AJ421150	6/10
Chilomonas sp.	M1303	WARIS-H	AJ420676	*AJ007276*	4/—
Chroomonas sp.	SAG B 980-1	WARIS-H	AJ420677	AJ420698	5/9
Chroomonas sp.	M1312	WARIS-H	AJ420678	*AJ007277*	1/—
Chroomonas sp.	M1318	ASP-H	AJ420679	*AJ007279*	1/—
Chroomonas sp.	M1481	WARIS-H	AJ420680	*AJ007278*	5/—
Chroomonas sp.	M1703	ASP-H	AJ420681	*AJ420699*	5/10
Cryptomonas sp.	M0420	WARIS-H	AJ420682	*AJ007280*	3/—
Cryptomonas sp.	M0739	WARIS-H	AJ420683	AJ420697	4/3
Cryptomonas ovata var. *palustris*	CCAP 979/61	WARIS-H	AJ420684	AJ421147	5/10
Cryptomonas sp.	M1094	WARIS-H	AJ420685	*AJ007281*	3/—
Cryptomonas sp.	M1079	WARIS-H	AJ420686	AJ421149	5/10
Cryptomonas sp.	M1171	WARIS-H	AJ420687	AJ420695	3/10
Cryptomonas compressa	SCCAP K-0063 Fada	WARIS-H	AJ420688	AJ420696	1/10
Falcomonas daucoides	ShP-CSUCC	(Not cultivated)	AJ420689	*AF143943*	3, 6/—
Hemiselmis refescens	CCMP 439	ESM	AJ420690	*AJ007283*	2/—
Hemiselmis virescens	CCMP 443	ESM	AJ420691	*AJ007284*	3/—
Porphyridium aerugineum	SAG 43.94	WARIS-H/ESM		AJ421145	—/11
Proteomonas sulcata	CCMP 704	ASP-H 28	AJ420692	*AJ007285*	7, 8/—
Rhodomonas sp.	M1480	ASP-H	AJ420693	*AJ007286*	3/—
Rhodomonas sp.	M1630	ASP-H 28	AJ420694	AJ421148	5/10
Teleaulax amphioxeia	SCCAP K-0434	ESM	AJ421146	*AJ007287*	3/—

[a] The primer combinations used in the PCR reactions are listed in Table 2. CCAP, Culture Collection of Algae and Protozoa (UK); CCMP, Center for Culture of Marine Phytoplankton (USA); M, Culture Collection Melkonian (Cologne, Germany); SAG, Sammlung von Algenkulturen at Göttingen (Germany); SCCAP, Scandinavian Culture Collection of Algae and Protozoa (Denmark); num, nucleomorph; nuc, nucleus; ASP-H 28, ASP-H with 28 g/L NaCl.

[b] Accession number in italics: sequence published elsewhere.

were determined with a Li-Cor 4000L automated sequencer using 66-cm plates.

In strain *Proteomonas sulcata* (CCMP 704) no nucleomorph-specific primer combination (combinations 1 to 6; Table 2) led to a specific PCR product, thus the PCR was performed in two steps. First, a new PCR primer ProtNM2F was constructed by comparison of a nucleomorph SSU rDNA consensus sequence (inferred from all other nucleomorph sequences) with the nuclear SSU rDNA from the same strain (Table 2). A combination with primer BR, a lower annealing temperature (55°C), an addition of 2% DMSO, and a reamplification resulted in a 3′ fragment of 1000 bp of the *P. sulcata* nucleomorph (primer combination 7; Table 2). This fragment was sequenced and used to construct a reverse primer (by comparing a nuclear SSU rDNA consensus sequence inferred from all nuclear sequences to the nucleomorph fragment of *P. sulcata;* Table 2), PsulcNM1R, to obtain the 5′ part of the CCMP 704 nucleomorph SSU rDNA (primer combination 8; Table 2). Since the 5′ part of the sequence was ambiguous due to the presence of a second product, a nonbiotinylated version of the PCR product was cloned. The PCR product was purified prior to cloning by agarose gel electrophoresis. The gel slices were treated with the QiaQuick Gel Extraction Kit (Qiagen). The eluted products were concentrated by precipitation (200 μl eluate, 500 μl absolute ethanol, 20 μl 3 *M* Na-acetate, pH 5.2, 2 μl 20 mg/ml glycogen; −20°C for 30 min), washed twice in 80% ethanol, and dissolved in 5 μl H_2O. For cloning, Ca^{2+}-competent *E. coli* cells (Inoue et al. 1990; strain DH5α), the TaKaRa DNA Ligation Kit Version 1 (TaKaRa Shuzo Co. Ltd), and the pGEM TEasy vector (Promega) were used. Clones were grown on LB agar plates [100 μg cAMP/ml, 40 μl 2% X-gal in DMSO (Sambrook et al. 1989)]. Plasmid DNA was purified using the GFX Micro Plasmid Prep Kit (Amersham Pharmacia) and sequenced using the primer T7 and the standard SSU rDNA primers mentioned above. To compensate for Taq polymerase reading errors, several clones were sequenced.

In strain Fada ShP-CSUCC (*Falcomonas daucoides*), polymerase slippage during PCR ("roller-coasting") made sequencing reactions unreadable due to homopolymers of A and T in two highly variable regions of the nucleomorph SSU rDNA. Since neither forward nor backward reactions crossed these regions, this part of the sequence could not be assembled by direct sequencing of the PCR product. To solve the problem, a nonbiotinylated PCR product was cloned and sequenced as described above.

Phylogenetic Analyses

The SSU rDNA sequences were aligned manually with the multiple sequence alignment editor Seaview (Galtier et al. 1996). The *Komma caudata* nucleomorph SSU rDNA sequence (accession No. U53121) was excluded from the nucleomorph alignments due to the large number of ambiguous sites. Phylogenetic analyses were performed with the program PAUP* 4.0beta [portable version under Debian 2.2 GNU/Linux for Alpha processors and MacOS PPC version, updated during analyses from 4.0b4a, 4.0b4b to 4.0b8 (Swofford 1998)]. Nonalignable regions were excluded prior to the analyses. Six data sets were subjected to phylogenetic analyses: a large rhodophyte alignment (123 SSU rDNA sequences including the nucleomorph sequences, Viridiplantae as outgroup taxa), a nucleomorph alignment of 47 sequences (Bangiophyceae as outgroup taxa), a nuclear alignment with 39 sequences (Glaucocystophyta as outgroup taxa), and three data sets without outgroup and equal taxon sampling for direct comparison of the tree topologies (termed combined, nucleomorph-only, and nucleus-only

Table 2. PCR and sequencing primers[a]

PCR primers	
Designation	Sequence (5′ to 3′)
Nucleomorph-specific primers	
CrNM1F (biot.)	CAGTAGTCATATGCTTGTCTTAAG
NMITS044R	GTTGCTTGGGAGTGCAGCTC
NMITS055R	CTTGGTCCGTGTTTCAAGACGGGTC
ProtNM2F	GTGAAYAAAWTAGAGTGTTCATG
PsulcNM1R	GCACCGGGGCCAGCGATCCGACCAC
Nucleus-specific primer	
CrN1F	CTGCCAGTAGTCATATGCTTGTCTC
Common primers	
AF (biot.)	CCGAATTCGTCGACAACCTGGTTGATCCTGCCAGT
BR	CCCGGGATCCAAGCTTGATCCTTCTGCAGGTTCACCTAC
ITS055R (biot. or nonbiot.)	CTCCTTGGTCCGTTTCAAGACGGG

Primer combinations used in PCR (primary/seminested reamplification)	
Combination	Primer combination No.
CrNM1F (biot.)–BR	1
CrNM1F (biot.)–ITS055R	2
CrNM1F (biot.)–ITS055R/CrNM1F (biot.)–BR	3
AF (biot.)–NMITS055R	4
AF (biot.)–NMITS044R	5
AF (biot.)–NMITS044R/AF (biot.)–BR	6
ProtNM2F–BR (biot.)	7
AF–PsulcNM1R	8
CrN1F–ITS055R (biot.)	9
CrN1F–BR (biot.)	10
AF–ITS055R (biot.)	11

Sequencing primers	
Designation	Sequence (5′ to 3′)
AF	CGTCGACAACCTGGTTGATCCTGCC
82F*	GAAACTGCGAATGGCTC
300F	GGAGAATTAGGGTTCGATTCCGGAG
528F*	CGGTAATTCCAGCTCC
920F*	GAAACTTAAAKGAATTG
BR*	TTGATCCTTCTGCAGGTTCACCTAC
920R*	ATTCCTTTRAGTTTC
NM690R	TCCAAGAATTTCACCTCTG
536R*	GWATTACCGCGGCKGCTG
E300R	GGCTCCCTCTCCGGAATCRAACCC

[a] All sequencing primers are labeled at their 5′ terminus with an 800-nm IR-fluorescent dye (MWG Biotech). The PCR primers NMITS044R, NMITS055R, ProtNM2F, and PsulcNM1R and the sequencing primer NM690R were newly constructed for this study. The sequencing primer E300R was designed for euglenophyte SSU rDNA sequences (Marin et al., in preparation). All other primers have been introduced elsewhere (Elwood et al. 1985; Medlin et al. 1988; Cavalier-Smith et al. 1996; Marin et al. 1998). PCR combinations with the primer CrNM1F were supposed to result in nucleomorph SSU rDNA products, but in some cases this primer turned out to be nonspecific and amplified nuclear SSU rDNA (see Table 1, strain M0739). F, forward primer; R reverse primer; (biot.), biotinylated at the 5′ terminus. * Standard sequencing primers. The primers without asterisks were used when problems were encountered to obtain a continuous and double-stranded sequence.

data sets in this study; all alignments are available from the authors upon request). All taxa not present in both data sets were deleted from the alignments (see Results for details). The data sets of the combined alignments finally comprised 30 taxa. In the combined data set, nucleomorph and nuclear SSU rDNA sequences were joined to one alignment. For taxon sampling and accession numbers of sequences from DDBJ/EMBL/GenBank, see Figs. 2–4. Accession numbers of new sequences are listed in Table 1.

As outgroup taxa for the large rhodophyte alignment, several chlorophyte and streptophyte nuclear sequences were chosen, since in previous studies the chlorophytes clustered as a sister to the red algal lineage (Moreira et al. 2000; Van de Peer et al. 2000). The outgroup taxa for the nucleomorph alignment were chosen according to the results of the phylogenetic analyses performed on the rhodophyte data set (see Results). Nuclear SSU rDNA sequences of the Glaucocystophyta, the closest known relatives to the cryptophyte host cells (Bhattacharya et al. 1995; Van de Peer et al. 2000), were used as an outgroup to the nuclear sequences of the cryptophytes.

To test for homogeneity of base frequencies across taxa, the empirical base frequencies of the nucleomorph and nuclear SSU rDNA

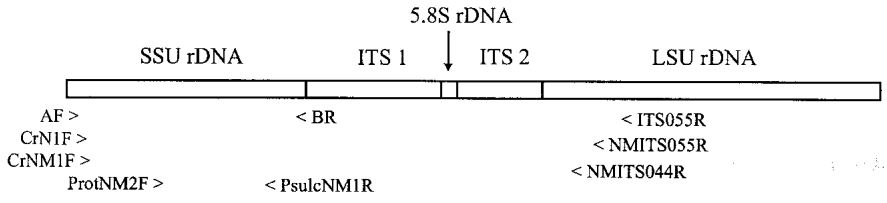

Fig. 1. Approximate positions (*arrowheads*) of the PCR primers used in this study. For sequences and primer combinations see Table 2.

sequences were determined by applying the command "basefreqs" implemented in PAUP* 4.0beta (Swofford 1998).

Each data set and each modified data set (e.g., by excluding single taxa or complete clades) was tested with Modeltest 3.04 to find the model of evolution fitting the data best (Posada and Crandall 1998). The different data sets were subjected to maximum-likelihood analyses, using the evolutionary model proposed by Modeltest from the hierarchical likelihood-ratio tests (hLRT) (Felsenstein 1981; Goldman 1993), except for the large rhodophyte alignment, because of restrictions of computation time. The data sets were also analyzed by using the maximum-likelihood estimators of the proposed evolutionary model to calculate distances for neighbor-joining trees (Saitou and Nei 1987). In addition, unweighted parsimony analyses were performed (Fitch 1977) (addition sequence, random; 10 replicates; heuristic search). Bootstrap analyses were run under the distance criterion (distances calculated using the maximum-likelihood settings; see above) and under the parsimony criterion [1000 replicates for both distance and parsimony criteria (Felsenstein 1985)]. For the parsimony bootstrap analysis of the rhodophyte alignment it proved necessary to remove 14 sequences, which were almost-identical to others prior to the analysis, and only 500 replicates were done (deleted sequences with accession numbers as follows: *Rhodosorus* sp., AF168626; *Goniotrichopsis sublittoralis,* AF168629; *Stylonema alsidii,* AF168633; *Stylonema cornu-cervi,* AF168622; *Porphyridium aerugineum,* SAG 43.94; *Porphyridium aerugineum,* AF168623; *Compsopogonopsis leptoclados,* AF087123; *Chroomonas* sp., CCAC M1703; *Hemiselmis rufescens,* CCMP 439; *Chroomonas* sp., X81327; *Rhinomonas pauca,* U53131; *Porphyra tenera,* AB013176; *Porphyra amplissima,* L36084; *Plocamiocolax pulvinata,* U09618). Bootstrap analyses under the maximum-likelihood criterion (100 replicates) were performed only with the three data sets of the combined analyses.

Kishino–Hasegawa Tests (KHTs)

To test the effects of transferring single taxa or clades to different positions, user-defined or constraint trees were compared with optimal trees derived from the maximum-likelihood analyses. Minor modifications requiring changes of only single branches were done with TreeviewPPC 1.66 (Page 1996). In one rearrangement (CRYP sorted; see Table 3), more than one branch had to be moved. To avoid a suboptimal structure in the strongly modified new subclades, the topology of the tree was optimized under the maximum-likelihood criterion using the constraint function implemented in PAUP 4.0beta. All user-defined and constraint trees for a specific data set were combined into one treefile and subjected to KHTs.

To compare directly the tree topologies of the combined, nucleomorph-only, and nucleus-only alignments, the maximum-likelihood trees of each data set were combined into one treefile and tested against each of the three data sets.

The setup of the treefiles for the KHTs are listed and further explained in Tables 3 and 4. The KHTs were performed using PAUP 4.0b8 [RELL method, 1000 bootstrap replicates, one-tailed (Kishino and Hasegawa 1989; Swofford 1998; Goldman et al. 2000)]. For all KHTs the evolutionary model GTR + Γ + *I* was used to accommodate the different data sets and tree topologies (Rodríguez et al. 1990).

Spectrophotometry

The biliproteins of strains M1630, M1709, and SAG B 980-1 were determined as described by Hill and Rowan (1989) and Marin et al. (1998). The biliproteins of strains M1171, M1079, M0739, and SCCAP K-0063 have been identified elsewhere (Hoef-Emden and Melkonian, in preparation).

Results

Characteristics of the Nuclear and Nucleomorph SSU rDNA Sequences

The lengths of the nuclear SSU rDNA sequences obtained ranged from approximately 1700 to 1800 nucleotides (nt); the nucleomorph SSU rDNA sequences were slightly longer (approx. 1800 to 2050 nt). Base frequencies across taxa were found to be homogeneous for the complete nuclear SSU rDNA sequences (including the outgroup taxa and nonalignable regions) but not for the complete nucleomorph sequences. However, with the exclusion of the nonalignable regions, the nucleomorph SSU rDNA sequences passed the homogeneity test (complete taxon setup, including outgroup taxa). These parts of the sequences were alignable and, thus, could be used for phylogenetic analyses.

Evolutionary Models Proposed by Modeltest

For all data sets, Modeltest proposed complex evolutionary models with among-site substition rate variation (gamma distribution; Γ) and proportion of invariable sites (*I*).

The Rhodophyte Data Set

The large rhodophyte alignment was assembled (for details see Materials and Methods) to reveal red algal lineages which are closely related to the origin of the cryptophyte plastid and to select an appropriate set of rhodophyte sequences as an outgroup for the more detailed analyses with the nucleomorph alignment. To optimize the taxon sampling and to cover the biodiversity of the Rhodophyta, taxa were chosen to represent different orders of the Bangiophyceae (Bangiales, Compsopogonales, Porphyridiales, Rhodochaetales) and of the Florideophyceae (Acrochaetiales, Ahnfeltiales, Ba-

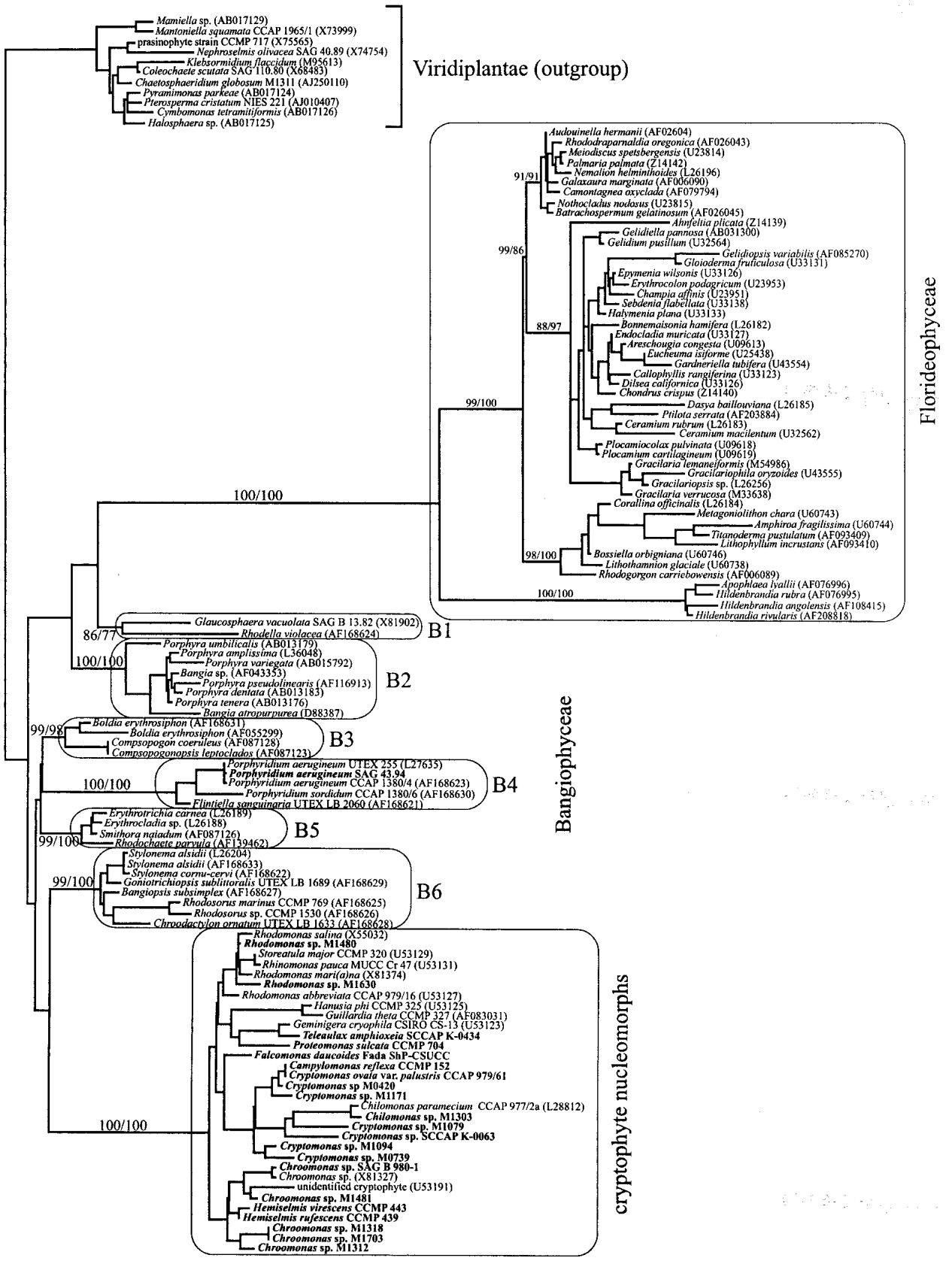

Fig. 2. Rooted distance/neighbor-joining tree of the rhodophyte alignment with nuclear SSU rDNA sequences of Viridiplantae as outgroup. Taxa with strain designations, if available, and with accession numbers of the corresponding SSU rDNA sequences from EMBL/GenBank (in parentheses). The distances were calculated using the likelihood parameters estimated by Modeltest for the suggested evolutionary model [hierarchical likelihood-ratio tests (hLRT): Tamura–Nei (1993) with gamma distribution (Γ) and proportion of invariable sites (*I*)]. Bootstrap values: neighbor-joining with distance matrix calculated using the maximum-likelihood estimators of the suggested evolutionary model (1000 replicates) and unweighted maximum parsimony (500 replicates, reduced taxon sampling; see Materials and Methods; bootstrap values in order from left to right). Bootstrap values of the terminal clades not shown. Sequences determined in this study in *boldface.* B1–B6, bangiophycean lineages; scale bar, substitutions per site.

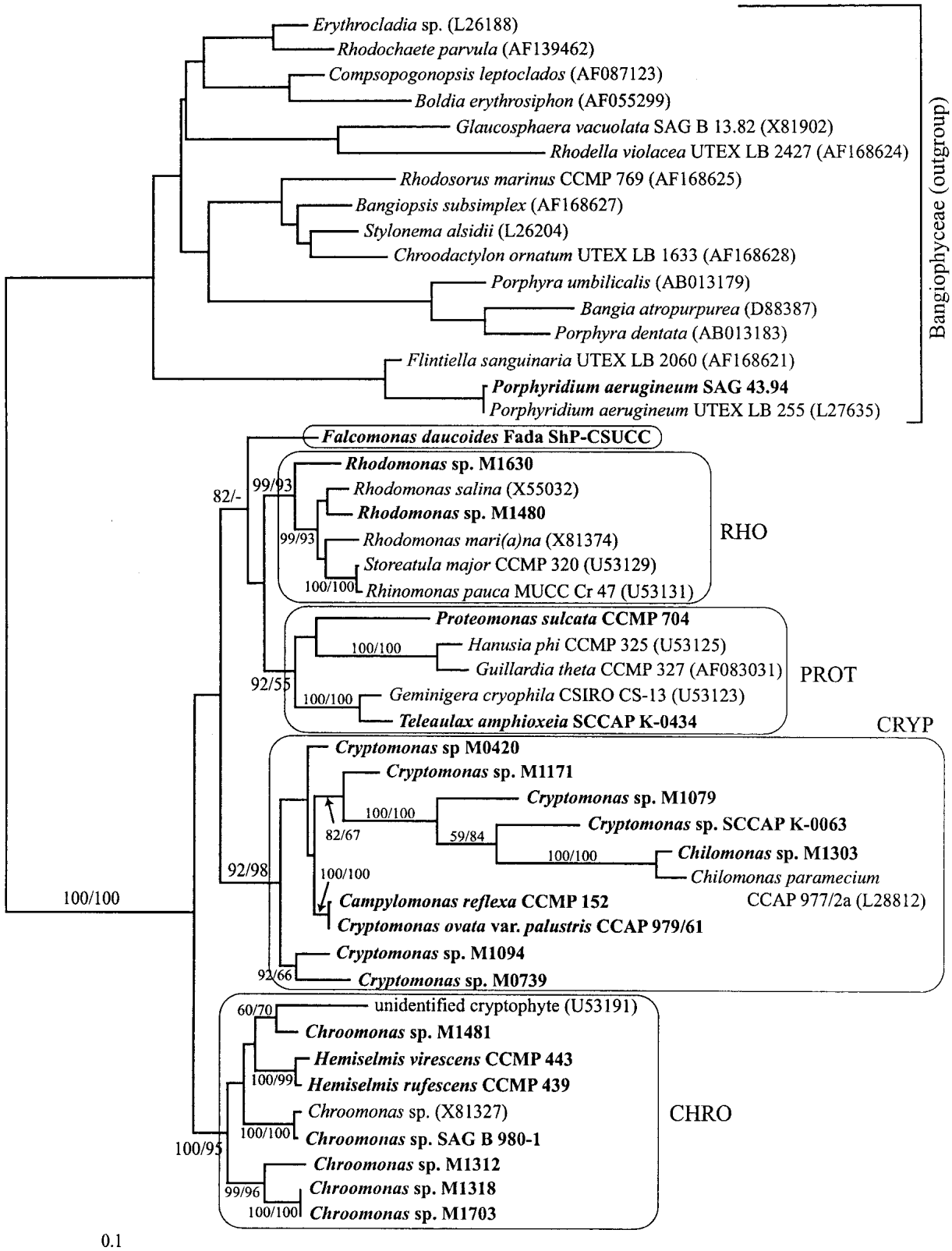

Fig. 3. Maximum-likelihood tree of the nucleomorph SSU rDNA data set of the cryptophytes rooted with selected bangiophycean nuclear sequences. Taxa with strain designations, if available, and with accession numbers of the corresponding SSU rDNA sequences from EMBL/GenBank (in parentheses). Evolutionary model as proposed by Modeltest (hLRT: Tamura–Nei with $\Gamma + I$). Bootstrap values (1000 replicates): neighbor-joining with distance matrix calculated using the maximum-likelihood estimators of the suggested evolutionary model and unweighted maximum parsimony (bootstrap values in order from left to right). Sequences determined in this study in *boldface*. $-\ln L = 12415.33289$; scale bar, substitutions per site.

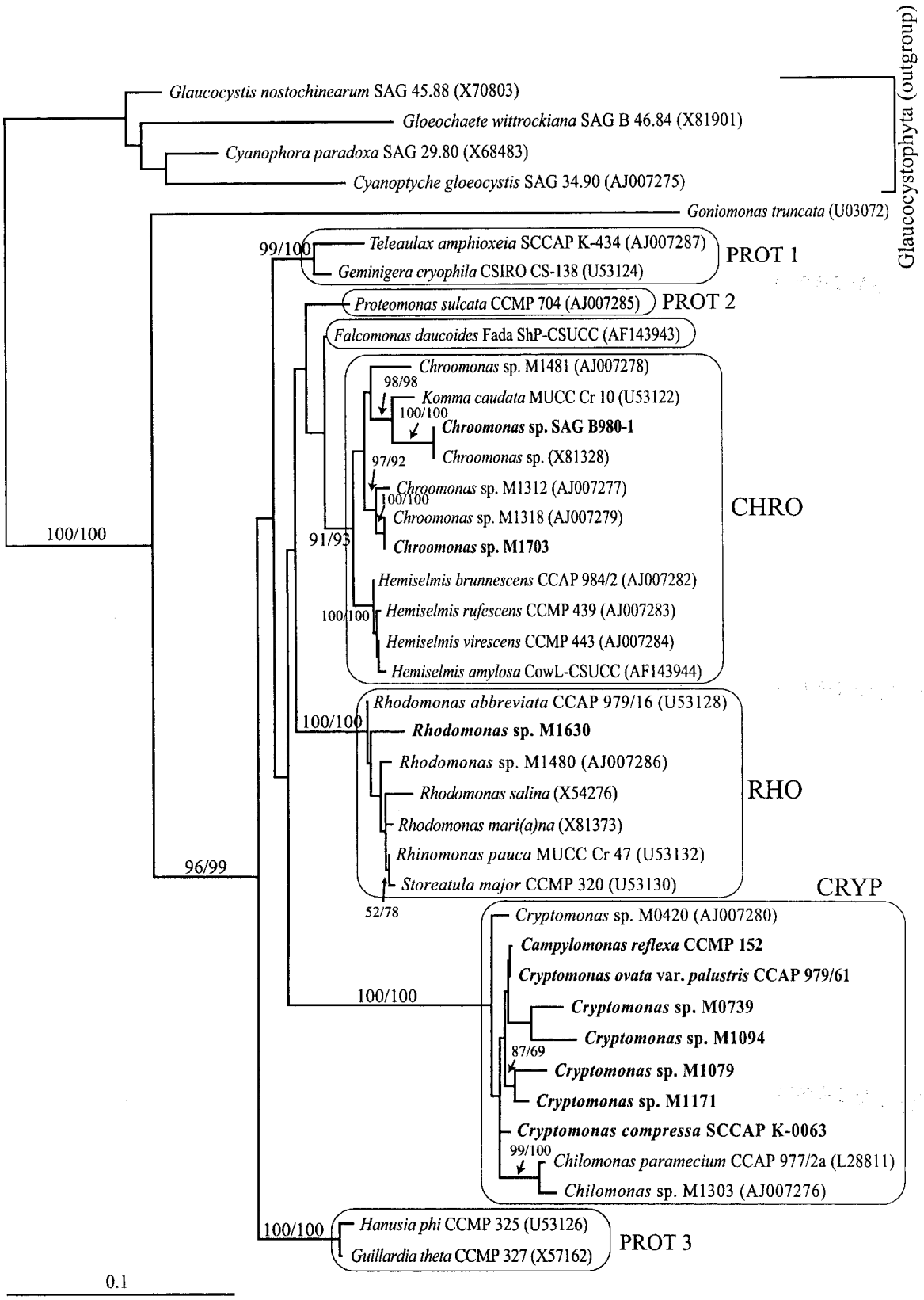

Fig. 4. Maximum-likelihood tree of the cryptophyte nuclear SSU rDNA data set rooted with glaucocystophyte nuclear SSU rDNA sequences (Tamura–Nei with $\Gamma + I$). Taxa with strain designations, if available, and with accession numbers of the corresponding SSU rDNA sequences from EMBL/GenBank (in parentheses). Bootstrap values (1000 replicates): distance matrix calculated using the maximum-likelihood estimators of the suggested evolutionary model (hLRT: Tamura–Nei with $\Gamma + I$) and unweighted maximum parsimony (bootstrap values in order from left to right). Sequences determined in this study in *boldface*. $-\ln L = 8411.47946$; scale bar, substitutions per site.

Table 3. Results of one-tailed Kishino–Hasegawa tests (probability values) performed on modifications of the maximum-likelihood trees depicted in Figs. 5A to C[a]

Modification	Nucleomorph-only	Combined	Nucleus-only
Unmodified (best)	Fig. 5A	Fig. 5B	Fig. 5C
Falcomonas → CHRO	0.114	—	—
Falcomonas → CRYP	0.123	0.115	**0.036**
Falcomonas → PROT	0.114	Ø	—
Falcomonas → RHO	0.114	**0.031**	0.145
Falcomonas → PROT 1 + 3	Ø	**0.031**	Ø
Falcomonas → PROT 1	Ø	Ø	**0.039**
Falcomonas → PROT 2 (*P. sulcata*)	Ø	0.119	0.349
Falcomonas → PROT 3	Ø	Ø	**0.036**
Proteomonas → *Falcomonas*	0.169	0.086	0.491
Proteomonas → CHRO	0.060	**0.049**	0.187
Proteomonas → CRYP	0.060	0.221	0.054
Proteomonas → PROT 1 + 3	—	0.358	—
Proteomonas → RHO	0.161	0.181	—
CRYP sorted[b]	**0.002**	**0.000**	**0.021**

[a] Each column represents one treefile; each row represents one type of modification of the optimal topology depicted in the figures listed in the first row (e.g., *Falcomonas* → RHO = *Falcomonas* as a sister to clade RHO); *boldface,* rejection of null hypothesis at probability values below 0.05; Ø, clade not present in tree or part of a larger clade; —, corresponds to topology of best tree, therefore not tested.

[b] CRYP sorted according to periplast type: strains with polygonal periplast plates (strains M0420, M0739, M1171, CCAP 979/61) separated from strains with sheet-like periplasts (M1094, M1079, CCAC M1303, CCAP 977/2a, CCMP 152, SCCAP K-0063; for a comparison see Fig. 6).

Table 4. Results of one-tailed Kishino–Hasegawa tests performed on the data sets of the combined analyses[a]

	Nucleomorph-only			Combined			Nucleus-only		
Topology	−ln*L*	Δ−ln*L*	*p*	−ln*L*	Δ−ln*L*	*p*	−ln*L*	Δ−ln*L*	*p*
Fig. 5A	7034.92790	(Best)		13272.43730	10.26131	0.187	6007.08192	43.28508	**0.003**
Fig. 5B	7052.54838	17.62048	0.066	13262.17599	(Best)		5993.74112	29.94428	**0.040**
Fig. 5C	7172.80539	137.87749	**0.0000**	13393.45297	131.27698	**0.000**	5963.79673	(Best)	

[a] Each data set is represented by three columns: −ln likelihood (−ln*L*), differences of −ln likelihood to the best tree (Δ−ln*L*), and probability values (*p*). Each row represents a different tree topology depicted in the appropriate figures listed in the first column. The tests were done using GTR + Γ + *I* settings.

trachospermales, Bonnemaisonniales, Ceramiales, Corallinales, Gelidiales, Gigartinales, Gracilariales, Halymeniales, Hildenbrandiales, Nemalionales, Palmariales, Plocamiales, Rhodogorgonales, Rhodymeniales).

Neighbor-joining (maximum-likelihood distance matrix) and maximum-parsimony analyses (480 equally parsimonious trees) resulted in eight well-supported groups (cryptophyte nucleomorphs, Florideophyceae, and six bangiophycean clades, B1–B6; Fig. 2). But even when the long-branched florideophycean clade was removed, the basal branching order of the trees could not be resolved. Thus from the topology of the trees, no specific bangiophycean clade can be deduced to be more closely related to the cryptophyte nucleomorphs than another. The outgroup taxa for the nucleomorph analyses were therefore chosen by taking two or three sequences from each of the six bangiophycean clades (Fig. 3).

The Nucleomorph Data Set

In all analyses of nucleomorph SSU rDNA sequences, cryptophyte taxa stably formed four clades plus one single taxon, *Falcomonas daucoides* (maximum-likelihood tree in Fig. 3; parsimony—six equally parsimonious trees, not shown). One clade comprised strains of *Rhodomonas, Rhinomonas,* and *Storeatula* (referred to henceforth as clade RHO). The *Rhodomonas abbreviata* nucleomorph sequence was excluded from all further analyses, since it showed suspicious deviations (e.g., repeatedly only one G instead of two G's as in all other cryptophyte sequences or substitutions in regions otherwise highly conserved throughout all sequences of the alignment). Removing the *Rhodomonas abbreviata* sequence resulted in an increased bootstrap support for the RHO clade, from 60 to 99% for the distance analysis and from 67 to 93% for the maximum-parsimony analysis. The second clade consisted of the genera *Guillardia, Hanusia, Geminigera, Teleaulax,* and *Proteomonas* (clade PROT). In the third clade all strains of *Hemiselmis* and *Chroomonas* were found (clade CHRO). The fourth clade consisted of *Cryptomonas, Chilomonas,* and *Campylomonas* sequences (clade CRYP).

In rooted trees (see Fig. 3), the basal topology was not resolved. However, when the outgroup taxa were ex-

cluded, the bootstrap frequencies for the internal nodes increased to significant levels (Fig. 5A), whereas omitting the long-branch taxa of clade CRYP (*Chilomonas,* M1079, and SCCAP K-0063 sequences; Figs. 3 and 5A) from the analyses did not significantly influence the bootstrap values.

The well-supported CRYP clade, comprising freshwater taxa only, showed the most conspicuous topology (Fig. 3): within this clade a long-branch subclade of four sequences emerged, indicating a higher evolutionary rate in this part of the tree. The two early-diverging sequences in this subclade belong to photoautotrophic strains assigned to the genus *Cryptomonas* (strains M1079 and SCCAP K-0063), whereas the two later-diverging sequences belong to strains of the heterotrophic genus *Chilomonas.* The branch common to the four taxa showed maximal support for all bootstrap analyses (100%). Among the short-branched CRYP sequences, the almost-identical sequences of strains CCMP 152 (the authentic strain of *Campylomonas reflexa*) and CCAP 979/61 ("*Cryptomonas ovata* var. *palustris*") formed a subclade supported by 100% bootstrap values for all three analyses.

The CHRO clade consisted of freshwater and marine strains assigned to the genus *Chroomonas,* two *Hemiselmis* strains, and an unidentified cryptophyte with a longer branch, resulting in *Chroomonas* being paraphyletic (Fig. 3). Three pairs of almost-identical sequences were found in this clade: *Hemiselmis rufescens/Hemiselmis virescens, Chroomonas* M1318/*Chroomonas* M1703, and SAG B980-1/*Chroomonas* accession No. X81327.

The PROT clade, with its comparatively short common branch but relatively long terminal branches, was well supported in the two distance analyses (rooted and unrooted; Figs. 3 and 5A) and in the unrooted maximum-parsimony analysis (Fig. 5A) but only weakly supported in the rooted maximum-parsimony and the unrooted maximum-likelihood analysis (Figs. 3 and 5A). Although the *Proteomonas sulcata* (CCMP 704) sequence was placed stably as a member of this clade in the distance and maximum-likelihood analyses, its position within the clade was uncertain, and depending on the type of analysis it was associated either with *Hanusia phi/Guillardia theta* or with *Teleaulax amphioxeia/Geminigera cryophila* (Figs. 3 and 5A).

In the RHO clade the paraphyletic *Rhodomonas* sequences were positioned at the base of the clade and two genera with nearly identical nucleomorph SSU rDNA sequences were located at the very tips (*Storeatula major* and *Rhinomonas pauca;* Figs. 3 and 5A).

The Nuclear Data Set

The alignment of the cryptophyte nuclear SSU rDNA sequences included the sequence of the phagotrophic and aplastidic *Goniomonas truncata,* which was positioned at the very base of the cryptophyte sequences in all analyses (maximum parsimony, 96 equally parsimonious trees; distance/neighbor-joining, not shown; maximum-likelihood tree in Fig. 4). The SSU rDNA sequence of *Goniomonas truncata* showed the highest divergence of all sequences, even compared with the outgroup (Glaucocystophyta).

Three of the four clades found in the nucleomorph phylogeny were also recovered in the nuclear SSU rDNA trees. The clades CHRO, RHO, and CRYP were supported by high bootstrap values in all analyses, but the PROT clade of the nucleomorph trees split up into three lineages, *Teleaulax/Geminigera* (PROT 1), *Proteomonas sulcata* (PROT 2), and *Hanusia/Guillardia* (PROT 3; Fig. 4).

The CRYP clade displayed the longest branch of all plastid-containing cryptophyte lineages, whereas, in contrast to the nucleomorph phylogeny, no long-branch subclade was present within this clade (compare Figs. 3 and 4 and Figs. 5A and C). In the maximum-parsimony analysis, CRYP diverged after *Goniomonas* but prior to all other plastidic cryptophytes. When applying complex evolutionary models (distance and maximum-likelihood analyses), this branch collapsed and the CRYP clade radiated together with the other plastid-bearing lineages from the unresolved basal nodes of the trees, whereas the position of *Goniomonas* remained stable (Fig. 4). When the potentially interfering long-branch sequences of *Goniomonas truncata,* CRYP, and the outgroup taxa were excluded, only in analyses with all these sequences deleted did the bootstrap support for the internal branches of the trees increase. The deletion of only the outgroup taxa and *Goniomonas truncata* resulted in a topology with unresolved internal nodes and still separated PROT 1 and PROT 3 clades (Fig. 5C). Without clade CRYP, PROT 1 and 3 were placed in one clade with moderate to high bootstrap support (not shown). But unlike in the nucleomorph SSU rDNA trees, the position of *Pro-*

Fig. 5. Unrooted maximum-likelihood trees of the combined analyses. For a comparison of tree topologies and relative branch lengths, the maximum-likelihood trees of the nucleomorph-only, of the combined, and of the nucleus-only data set are depicted on one page (for details of taxon selection, see Results). Taxa with strain designations given only for otherwise ambiguous taxon names. **A** Tree of the nucleomorph-only data set [evolutionary model: TVM with $\Gamma + I$ (Rodríguez et al. 1990)]. $-\ln L = 7034.95642$. **B** Tree of the combined data set [evolutionary model: GTR with $\Gamma + I$ (Rodríguez et al. 1990)]. $-\ln L = 13262.35924$. **C** Tree of the nucleus-only data set [evolutionary model: Tamura–Nei (1993) with $\Gamma + I$]. $-\ln L = 5965.44353$. Bootstrap values: distance matrix calculated using the maximum-likelihood estimators of the suggested evolutionary model (hLRT; 1000 replicates), unweighted maximum parsimony (1000 replicates), and maximum likelihood (1000 replicates; bootstrap values in order from left to right). Scale bars, substitutions per site.

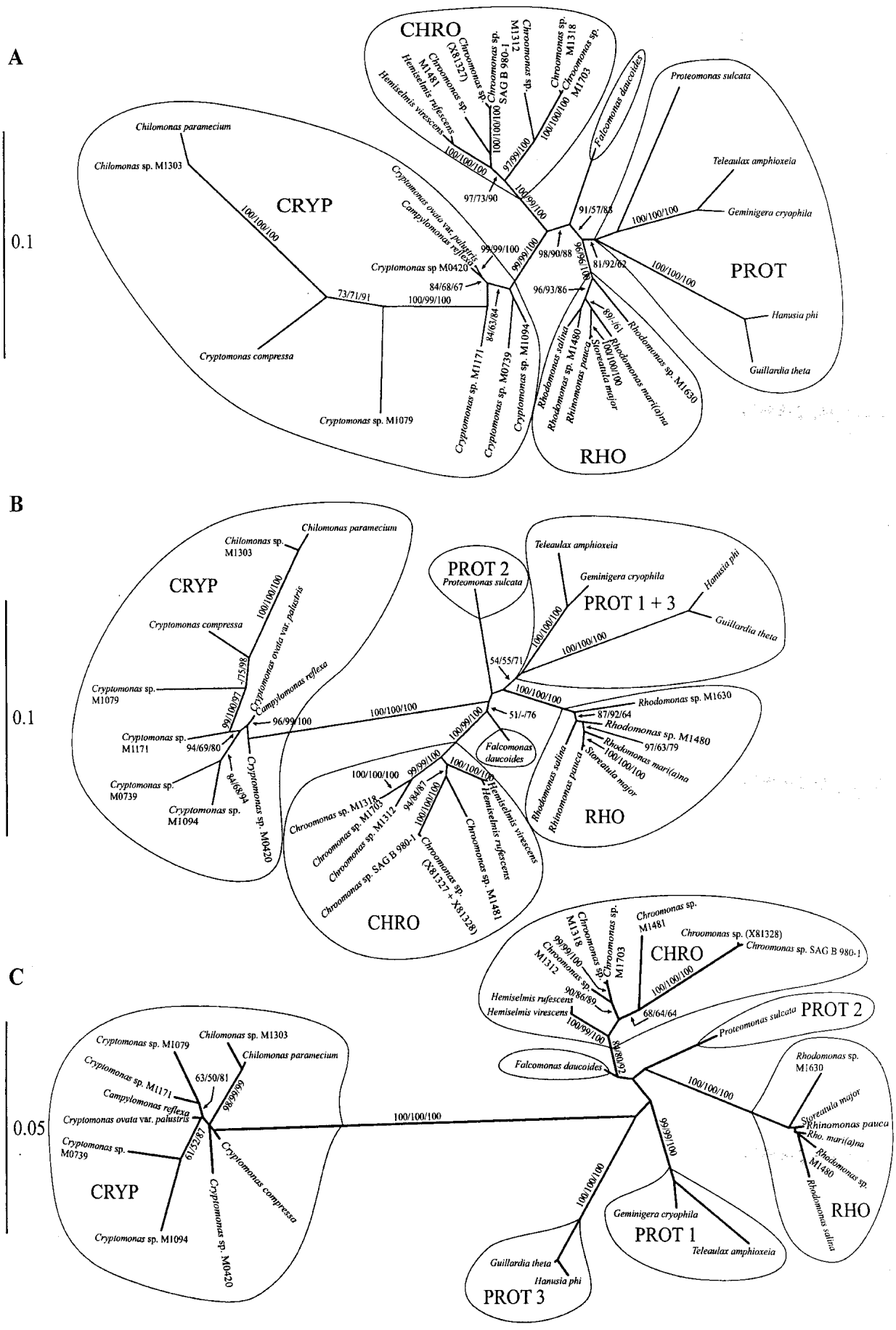
A
CHRO
CRYP
PROT
RHO
0.1
Chroomonas sp. (X81327)
Chroomonas sp. M1481
Hemiselmis rufescens
Hemiselmis virescens
Chroomonas sp. SAG B 980-1
Chroomonas sp. M1312
Chroomonas sp. M1318
Chroomonas sp. M1703
Falcomonas daucoides
Proteomonas sulcata
Teleaulax amphioxeia
Geminigera cryophila
Hanusia phi
Guillardia theta
Chilomonas paramecium
Chilomonas sp. M1303
Cryptomonas ovata var. palustris
Campylomonas reflexa
Cryptomonas sp M0420
Cryptomonas compressa
Cryptomonas sp. M1079
Cryptomonas sp. M1171
Cryptomonas sp. M0739
Cryptomonas sp. M1094
Rhodomonas salina
Rhodomonas sp. M1480
Rhinomonas pauca
Storeatula major
Rhodomonas mari(a)na
Rhodomonas sp. M1630
B
CRYP
PROT 2
PROT 1 + 3
CHRO
RHO
0.1
Chilomonas sp. M1303
Chilomonas paramecium
Cryptomonas compressa
Cryptomonas ovata var. palustris
Campylomonas reflexa
Cryptomonas sp. M1079
Cryptomonas sp. M1171
Cryptomonas sp. M0739
Cryptomonas sp. M1094
Cryptomonas sp. M0420
Proteomonas sulcata
Teleaulax amphioxeia
Geminigera cryophila
Hanusia phi
Guillardia theta
Falcomonas daucoides
Chroomonas sp. M1318
Chroomonas sp. M1703
Chroomonas sp. M1312
Chroomonas sp. SAG B 980-1
Chroomonas sp. (X81327 + X81328)
Hemiselmis virescens
Chroomonas sp. M1481
Rhodomonas sp. M1630
Rhodomonas sp. M1480
Rhodomonas mari(a)na
Storeatula major
Rhinomonas pauca
Rhodomonas salina
C
CRYP
CHRO
PROT 2
PROT 1
PROT 3
RHO
0.05
Cryptomonas sp. M1079
Chilomonas sp. M1303
Chilomonas paramecium
Cryptomonas sp. M1171
Campylomonas reflexa
Cryptomonas ovata var. palustris
Cryptomonas sp. M0739
Cryptomonas compressa
Cryptomonas sp. M0420
Cryptomonas sp. M1094
Chroomonas sp. M1318
Chroomonas sp. M1703
Chroomonas sp. M1481
Chroomonas sp. (X81328)
Chroomonas sp. SAG B 980-1
Chroomonas sp. M1312
Hemiselmis rufescens
Hemiselmis virescens
Falcomonas daucoides
Proteomonas sulcata
Geminigera cryophila
Teleaulax amphioxeia
Guillardia theta
Hanusia phi
Rhodomonas sp. M1630
Storeatula major
Rhinomonas pauca
Rho. mari(a)na
Rhodomonas sp. M1480
Rhodomonas salina

teomonas sulcata (PROT 2) remained separate from the PROT 1/PROT 3 clade and largely unresolved.

Within the CRYP clade a close association of *Cryptomonas ovata* var. *palustris* (strain CCAP 979/61) and *Campylomonas reflexa* (CCMP 152) was—as in the nucleomorph phylogenies—observed in the nuclear SSU rDNA trees (Figs. 4 and 5C).

In contrast to the topology of the nucleomorph SSU rDNA trees, the *Hemiselmis* sequences were gathered in a sister clade to the *Chroomonas/Komma* sequences (the latter, however, were not supported as a subclade; Fig. 4).

The Combined Analyses

In the combined analyses the tree topologies of the nuclear (1692 positions), of the nucleomorph (1509 positions), and of a combined data set with joined nuclear and nucleomorph SSU rDNA sequences (3201 positions) were directly compared and subjected to KHTs. To allow for a direct comparison of the trees, the data sets needed to be equated, i.e., the number of taxa and the taxon sampling had to be the same for all three data sets. Thus, all taxa not present in the nuclear and nucleomorph phylogenies were deleted. This elimination included the outgroups (Bangiophyceae in the nucleomorph data set, Glaucocystophyta in the nuclear data set), the sequences not present in the nucleomorph data set (*Goniomonas truncata* is aplastidic and, hence, has no nucleomorph; for *Hemiselmis amylosa, Hemiselmis brunnescens* nucleomorph SSU rDNA sequences were not available; the *Rhodomonas abbreviata* and *Komma caudata* nucleomorph SSU rDNA sequences were excluded due to ambiguities or substitutions in positions otherwise conserved throughout the data sets; see Materials and Methods and the results of the nucleomorph analyses above), and the sequences not present in the nuclear data set (the unidentified cryptophyte, accession No. U53191). The maximum-likelihood trees of the three data sets are depicted in Figs. 5A to C.

In the nucleomorph-only phylogeny, most internal nodes were supported by high bootstrap values (Fig. 5A). The maximum-parsimony analysis (six equally parsimonious trees) and the distance analysis resulted in the same clades and internal branching order as in the maximum-likelihood topology (results not shown).

In the nucleus-only alignment, clade PROT split up into three lineages, PROT 1 to 3 (Fig. 5C), as in the larger nuclear data set (Fig. 4). The setup of the clades remained the same, but the internal nodes of the tree again were not supported (Fig. 5C).

In the combined alignment, the additive effects of the joined nucleomorph and nuclear SSU rDNA sequences became obvious (Fig. 5B). The long basal branch of the nuclear CRYP clade and the long branches of the subclade containing the two *Chilomonas* sequences (see Fig. 5A) within the nucleomorph CRYP clade became shorter in the combined topology as is evident from a comparison of Figs. 5A and C. PROT 1 and 3 were gathered into one clade with a short common branch and low (distance and maximum parsimony) to moderate (maximum likelihood) bootstrap support (Fig. 5B). But the information added by the nucleomorph SSU rDNA did not place *Proteomonas sulcata* (PROT 2) in this clade; it still remained separated (only in maximum likelihood–distance was clade PROT present, supported by a bootstrap value of 70%; not shown). In the combined alignment no bootstrap support for internal nodes was observed, except for a sister-group relationship between *Falcomonas* and CHRO in the maximum-likelihood analysis (76%; Fig. 5B).

User-Defined and Constraint Trees

In the different data sets (Table 3), the position of the taxon *Falcomonas daucoides* and the incompletely resolved position of *Proteomonas* were examined. Additionally, in one constraint tree morphological characters (type of periplast; see also Fig. 6) were taken into account in the rearrangements, placing—according to their morphology—randomly distributed taxa into monophyletic clades. The results of the KHTs on tree modifications of the maximum-likelihood trees are listed in Table 3.

In the best tree in the nucleomorph-only data set in Fig. 5 *Falcomonas daucoides* was positioned centrally, separating the four clades into two pairs (CHRO/CRYP and RHO/PROT). Modifying these trees by transferring *F. daucoides* to the base of each of the four clades resulted in worse trees (p values: 0.114–0.123), although the p values were not below the significance threshold (0.05). In contrast, in the nucleus-only and combined SSU rDNA phylogenies (Figs. 5B and C), the position of *F. daucoides* seems to be more restricted, presumably due to its short branch. Changes in position were significantly worse for *F. daucoides* as a sister to CRYP, PROT 1, or PROT 3 in the nuclear phylogeny, whereas in the combined data set placement of *F. daucoides* next to RHO and PROT 1 + 3 was rejected.

The p values for separating *Proteomonas sulcata* from PROT in the nucleomorph-only tree (Fig. 5A) and placing it as a sister taxon to the three other clades depended on the evolutionary distance of the clades from PROT but, in no case, were below the significance threshold (Table 3). In the nucleus-only tree (Fig. 5C) the position of *Proteomonas* (PROT 2) was less defined: a monophyly of *Proteomonas* and *Falcomonas* was accepted with nearly 50% probability. In the combined data set (Fig. 5B, Table 3), the position of *Proteomonas* was also poorly defined, but a *Proteomonas*/CHRO sister group was rejected (Table 3).

In none of the three data sets tested did joining *F. daucoides* and *P. sulcata* into one clade result in a rejection of this topology.

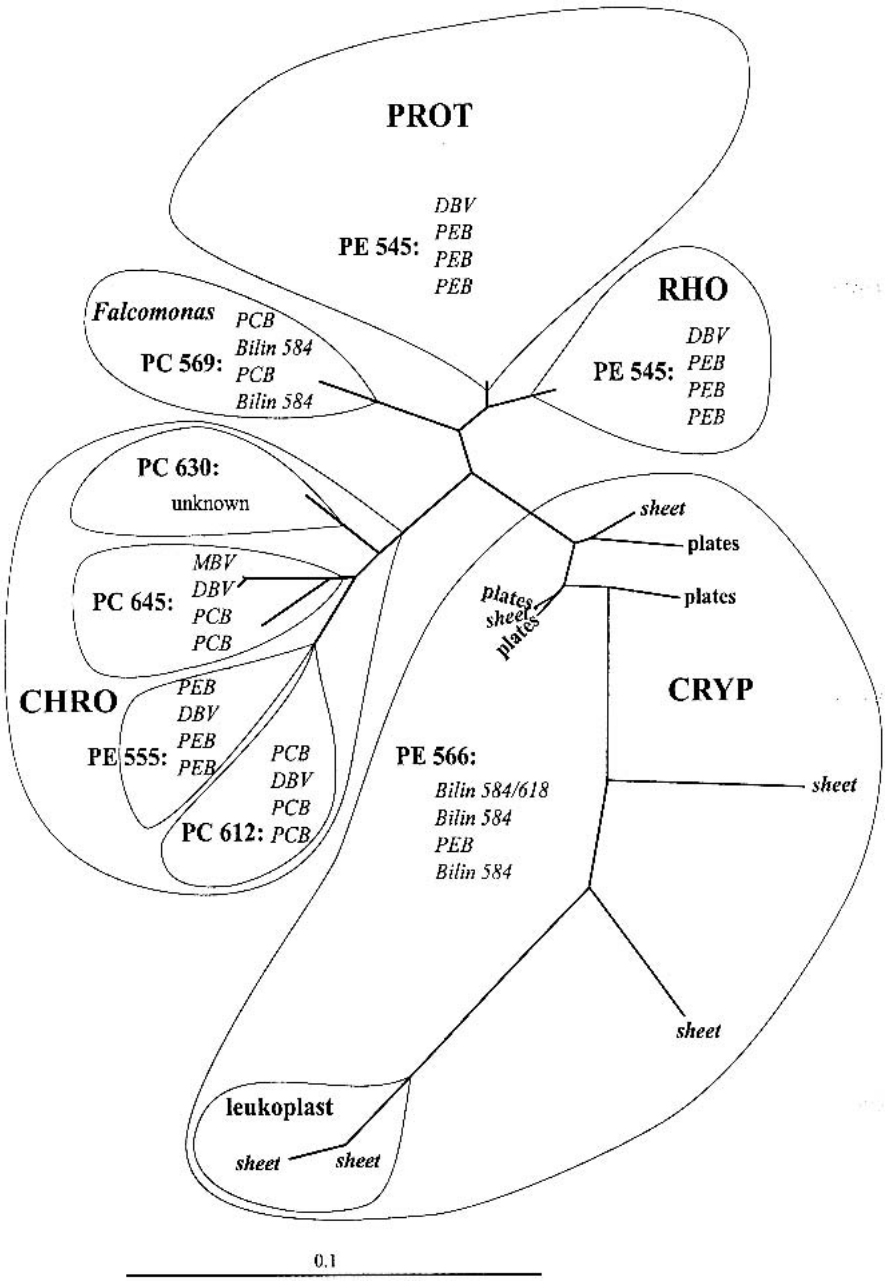

Fig. 6. Maximum-likelihood tree of the nucleomorph-only data set (see Fig. 5A) with biliprotein types and type of periplast (type of periplast: clade CRYP only) mapped onto the clades. PE, phycoerythrin; PC, phycocyanin. Absorption maxima: PE 545 at approx. 545 nm (shoulder at 560 nm), PE 555 at approx. 555 nm, PE 566 at approx. 566 nm (shoulder at 530 nm), PC 569 at approx. 569 and 630 nm (*underlined*—dominating maximum in the phycocyanins), PC 612 at approx. 580 and 612 nm, PC 630 at approx. 580 and 630 nm, PC 645 at approx. 580 and 645 nm [shoulder at 625 nm (Hill and Rowan 1989)]. Leucoplast—no pigmentation. Tetrapyrrolic chromophores (for each type of biliprotein positions listed from top to bottom in the order α-Cys-18(19), β-DiCys-50,61, β-Cys-82, β-Cys-158): Bilin 584 and 618, acrylobilins with corresponding absorption maxima; DBV, dihydrobiliverdin; MBV, mesobiliverdin; PCB, phycocyanobilin; PEB, phycoerythrobilin (Glazer and Wedemayer 1995). Inner periplast components in clade CRYP: plates, polygonal periplast plates; sheet, sheet-like (Hill 1991a). Scale bar, substitutions per site.

Results of the Kishino–Hasegawa Tests on Unmodified Trees of the Combined Analyses

The KHT results of the combined, the nucleomorph-only, and the nucleus-only maximum-likelihood tree topologies (Figs. 5A–C, combined into one treefile) against each of the three alignments are listed in Table 4.

When testing the nucleomorph-only and the combined alignment against the treefile, the nucleus-only tree topology was always rejected as significantly worse, whereas the topology of the combined alignment was not significantly worse than the nucleomorph-only data set, and vice versa. A different situation was found when the nucleus-only alignment was tested; both other trees—the nucleomorph-only tree and the tree of the combined data set—were rejected. Apparently, the sequences of the nucleomorph dominated over the nuclear signal in the combined alignment.

Discussion

Nuclear and Nucleomorph Tree Topologies: Congruences, Differences, and Difficulties

The two eukaryotic SSU rDNA phylogenies show obvious congruences in their tree topologies: three clades can be stably reconstructed irrespective of the chosen method of analysis in the nucleomorph and nuclear data sets,

strongly suggesting monophyletic groups in the cryptophytes (CHRO, CRYP, RHO). A fourth clade (PROT) is found as a stable structure in the trees inferred from the nucleomorph SSU rDNA sequences but could only be partially reconstructed in the nuclear trees (PROT 1 + 3) by excluding long-branch taxa from the analyses (when CRYP was deleted from the analyses; not shown). Despite the similar topology of the terminal clades, the nuclear and the nucleomorph SSU rDNA sequences differed markedly in the base frequencies of the complete alignments and in the base substitution rates. These results indicate that although coevolving in one group of organisms, the two eukaryotic SSU rDNAs are not necessarily subjected to the same selective forces.

The two long-branch nuclear ingroup lineages (*Goniomonas truncata* and CRYP) are obvious candidates for long-branch attraction (LBA) artifacts (e.g., Philippe 2000; Philippe et al. 2000). Not only the parsimony and distance methods are vulnerable to false-positive similarities caused by increased homoplasies, but also the maximum-likelihood method, in particular, when inappropriate evolutionary models are applied to the dataset in question (Felsenstein 1978; Hillis et al. 1994; Huelsenbeck 1995; Yang 1996). To detect possible LBAs, Bruno and Halpern (1999) suggested comparing tree topologies derived from simple and complex evolutionary models as a test for biased topologies. A biased topology under simple evolutionary models is demonstrated for the cryptophyte nuclear SSU rDNA phylogeny in this study. In trees constructed assuming equal rates in among-site rate variation, clade CRYP diverged prior to all other plastid-bearing lineages [Marin et al. (1998), CRYP labeled clade I; Clay and Kugrens (1999), CRYP labeled "A"; this study)]. As soon as a gamma-distributed among-site rate variation and a proportion of invariable sites are taken into account, this branch collapses and CRYP radiates together with the other plastid-bearing lineages from a nonresolvable tree base (this study).

A nonrandom addition of carefully selected taxa to break the long branches can help to decrease the influences of fast-evolving sequences (Hendy and Penny 1989; Graybeal 1998). From nuclear ITS 2 and partial LSU rDNA sequencing a closer association of the strains M1079 and SCCAP K-0063 to *Chilomonas* was suspected (Hoef-Emden, unpublished data), thus in this study the nucleomorph SSU rDNA sequences of these strains were added to the data sets to break successfully the long *Chilomonas* branch in the nucleomorph phylogeny (see Fig. 3). With respect to the CRYP clade in the nuclear SSU rDNA phylogeny, unfortunately a higher degree of divergence proved to be a synapomorphic feature of the complete nuclear clade CRYP. No related taxa with slower-evolving sequences suitable for substitution or to break the long basal branch leading to the CRYP clade could be found. The taxa in CRYP represent the most common freshwater cryptophytes, therefore excluding this clade from the analyses was not a desirable option.

As reported previously (e.g., Mahoney 2001) outgroups which are too distantly related to the ingroup decrease the resolution by adding homoplasies. In the nucleomorph data set, deleting the outgroup (the red algal class Bangiophyceae) was sufficient to reduce the influence of homoplasies and largely to resolve the internal branching order of the trees, whereas in the nuclear data set significant bootstrap values could be observed only for the internal branches when the three fast-evolving lineages [the outgroup (Glaucocystophyta), *Goniomonas truncata,* and CRYP] were excluded from the analyses (not shown). The influence of the extremely short branch of *Falcomonas daucoides* in the nuclear SSU rDNA trees is as yet unclear (see Figs. 4 and 5C). In few studies, disturbances by short branches similar to LBA were reported for maximum-parsimony and for neighbor-joining methods (Kim 1996; Kumar and Gadagkar 2000). However, a similarly short-branched second sequence to test for a possible "short-branch attraction artifact" was not present in the nuclear data set available.

Inadequate taxon sampling increases the topological bias caused by long-branch taxa in phylogenetic trees. In the first analyses of the nuclear and nucleomorph SSU rDNA phylogeny of cryptophytes (Cavalier-Smith et al. 1996), no representatives of the genus *Cryptomonas* were included in the analyses. As a consequence, *Chilomonas* emerged basal to all other plastid-bearing cryptophytes in both the nuclear and the nucleomorph phylogenies, and furthermore, in the nuclear phylogeny, *Chilomonas* clustered with *Goniomonas.* Marin et al. (1998) showed that the clustering of *Chilomonas* and *Goniomonas* in the nuclear phylogeny of Cavalier-Smith et al. (1996) was a LBA artifact caused by inadequate taxon sampling within clade CRYP. The results of this study revealed that the basal position of *Chilomonas* in the nucleomorph phylogeny of Cavalier-Smith et al. (1996) was also the result of an LBA artifact.

How Do the Long Branches Originate in the Cryptophytes?

Branch lengths in phylogenetic trees are a measure of divergence time and substitution rate (reviewed by Muse 2000). It is not straightforward to differenciate between branch lengths derived from an early divergence event and branch lengths caused by a higher substitution rate in isolated lineages.

In the nuclear SSU rDNA phylogeny, the position of *Goniomonas* remains basal when a complex evolutionary model is applied. *Goniomonas* is the only aplastidic and phagotrophic cryptophyte in the alignment and could have diverged prior to the aquisition of the complex plastid (McFadden et al. 1994b). Its position in the nuclear phylogeny as the most basal taxon is therefore plausible.

The strains in clade CRYP, however, show no obvious morphological or pigment features to support a more ancient origin than all other plastid-bearing cryptophytes (see below). The collapse of the basal CRYP branch under a complex evolutionary model strongly suggests the presence of homoplasies derived from a higher substitution rate. Explanations for a faster evolutionary rate within one lineage include so-called genetic bottleneck effects (Wu and Li 1985) or changes in nutritional mode (Nickrent and Starr 1994). Since CRYP is the only clade comprising exclusively freshwater taxa, it is conceivable that the taxa of CRYP may have originated from a small population of cryptophytes forced to adapt to freshwater and/or other environmental changes different from the occasional freshwater adaptations found in other lineages of cryptophytes [e.g., by being forced to migrate into deep water to survive grazers (Gervais 1998)].

In the colorless and osmotrophic genus *Chilomonas* leukoplasts are still present, but photosynthesis is lacking (Sepsenwol 1973). This seems to be accompanied by a higher substitution rate in the nucleomorph but not in the nuclear SSU rDNA, indicating a possible release of functional and hence structural constraints on the nucleomorph ribosomal operon.

The Cryptophyte Biliproteins: In Congruence with SSU rDNA Phylogeny

A correlation of the different cryptophyte biliprotein types with clades of the nuclear SSU rDNA phylogeny was reported previously (Marin et al. 1998; Clay and Kugrens 1999). In this study a correlation is found as well for the nucleomorph SSU rDNA phylogeny. For a better visualization the distribution pattern of the biliproteins is explained and mapped onto the nucleomorph tree in Fig. 6.

According to Hill and Rowan (1989) seven cryptophyte biliproteins, identifiable by their absorption spectra, are known and named after their dominating absorption maximum (see legend to Fig. 6). In most SSU rDNA clades only one type of biliprotein is found [CRYP—PE 566 or taxa lacking photosynthetic pigments, i.e., *Chilomonas;* RHO and PROT—PE 545 (Marin et al. 1998; Clay and Kugrens 1999; this study)]. The phycocyanin-dominated clade CHRO can be subdivided into lineages with PC 630, 645, 612, and one phycoerythrin (PE 555). *Falcomonas daucoides* contains PC 569.

The different absorption spectra are caused by a set of tetrapyrrolic chromophores covalently bound by one or two cysteinyl thioether linkages to the α (one chromophore) and β subunits (three chromophores) of the heterodimeric biliproteins (Glazer and Wedemayer 1995; see also Fig. 6).

Phylogenetic analyses showed that the β subunits of the cryptophyte biliproteins, irrespective of their blue or red color, are descendants of a rhodophyte phycoerythrin (Apt et al. 1995). The only presently known chromophore in the phycoerythrin of the Bangiophyceae is phycoerythrobilin (PEB) (reviewed by Apt et al. 1995), which is therefore most likely the ancestral character state of the cryptophyte biliprotein. In the cryptophytes this chromophore (PEB) dominates phycoerythrins 545 and 555 [three of four covalently bound chromophores are PEBs (Fig. 6) (Wedemayer et al. 1992; Wemmer et al. 1993)].

The positions of the outgroups in both cryptophyte SSU rDNA phylogenies depend on taxon sampling and the evolutionary model applied. This makes it impossible to determine which of the plastid-bearing clades represents the earliest-diverging lineage. Marin et al. (1998) suggested that PE 545 was the ancestral phycoerythrin in their clades II to VI [representing RHO, PROT 1–3, and CHRO and excluding the early-branching CRYP (their clade I)], since PE 545 appeared in four distinct lineages in their nuclear SSU rDNA phylogeny (Marin et al. 1998).

Although the position of the root could not be resolved, the basalmost lineages were often found to contain PE 545 (clades RHO and PROT; taxa predominantly from marine habitats). As discussed before, the chromophore setup of the PE 545 β subunit presumably represents the ancestral character state of the cryptophyte phycoerythrin, therefore clades RHO and PROT may be closer to the root of cryptophyte phylogeny than the other clades. We note that the tree topologies of the unrooted trees (Figs. 5A–C), which place RHO and PROT as sisters (in the nuclear tree after removal of CRYP; not shown), are compatible with such a view.

If the position of the root in the well-resolved unrooted nucleomorph SSU rDNA phylogeny is assumed to be at the base of RHO and PROT, the following scenario can be envisaged (Fig. 6): in the course of time a split into two lineages took place. In one branch, the chromophore of the α subunit was exchanged for DBV in the common ancestor of RHO and PROT [DBV is a precursor in the biosynthetic pathway of PEB and PCB in red algae and Cyanobacteria (Beale and Cornejo 1991; Cornejo and Beale 1997)]. In the other branch, leading to *Falcomonas,* CRYP and CHRO, first PCB and the acrylobilin Bilin 584 (Wedemayer et al. 1991) replaced PEB. The common ancestor of CRYP was separated by changing to freshwater habitats, lost PCB, and exchanged it for PEB and Bilin 584/618. CHRO evolved by the loss of the acrylobilins and by replacement with PCB and DBV. MBV (on the biliprotein α subunits of the PC 645 taxa; Fig. 6) may have arisen autocatalytically as reported for Cyanobacteria (Arciero et al. 1988; Zhao et al. 2000). Finally, a reversal took place to a red *Hemiselmis,* by exchanging all PCB chromophores with PEB. The nucleomorph tree topology implies that, unlike the situation in the nuclear phylogeny (Clay and Kugrens 1999; this study, *Falcomonas daucoides* is not at the basis of clade CHRO.

Cryptophyte Morphology and SSU rDNA Phylogeny

In addition to the biliprotein type, the systematics of the cryptophytes is based predominantly on ultrastructural characters such as the position of the nucleomorph, the periplast structure, the type of furrow/gullet system, and the flagellar root structures (Clay et al. 1999). Of these characters only the position of the nucleomorph shows congruence with the SSU rDNA phylogeny. Nucleomorphs embedded in the pyrenoid matrix are restricted to clade RHO (e.g., Gillott and Gibbs 1980; Cavalier-Smith et al. 1996; Marin et al. 1998; Clay et al. 1999; this study). In all other clades [except for *Geminigera cryophila:* nucleomorph in an invagination of the nucleus (Gillott and Gibbs 1980)] the nucleomorph is located free in the periplastidial space (Gillott and Gibbs 1980; Hill 1991a, b).

The furrow/gullet system, a cell invagination lined with large ejectisomes, shows only partial congruence with the tree topology: in CRYP, cells have a slit-like ventral opening, termed a furrow, in combination with a tubular invagination [gullet; reviewed by Clay et al. (1999) and Hoef-Emden and Melkonian (in preparation)], in CHRO, only gullets are found (e.g., Meyer and Pienaar 1984; Hill 1991b). In contrast to CRYP and CHRO, clade RHO morphologically is a mixture of taxa with a furrow–gullet combination [genus *Rhodomonas* (Hill and Wetherbee 1989)] or a gullet only [genera *Storeatula* and *Rhinomonas* (Hill and Wetherbee 1988; Hill 1991a)]. Similar differences are found in PROT in closely related taxa, e.g., *Hanusia* has a furrow, whereas *Guillardia* has a gullet (Deane et al. 1998).

A slightly different situation is found for the periplast type. The proteinaceous inner periplast component (IPC) located underneath the plasma membrane may be sheet-like or consist of distinct plates of different shapes [hexagonal, polygonal, rectangular, or staggered rectangular (Brett et al. 1994; Clay et al. 1999)]. The distribution of the IPC types (Fig. 6 as an example addressing the differing IPC types of CRYP) is incongruent with the molecular phylogeny. Fortunately isolates such as *Proteomonas sulcata* (Hill and Wetherbee 1986) and some *Cryptomonas* strains (Hoef-Emden and Melkonian, in preparation) offer an explanation: cryptophytes are potentially dimorphic. In the first report about dimorphism in a cryptophyte (Hill and Wetherbee 1986), the morphotypes of *Proteomonas sulcata* were introduced as diplomorph and haplomorph, implying the presence of a sexual life history, which has not yet been conclusively shown in any cryptophyte. Both morphotypes share the same type of cell invagination (a combination of furrow and gullet) and the same type of biliprotein (PE 545) but differ in the flagellar root system (long keeled rhizostyle vs. shorter nonkeeled rhizostyle) and in the type of inner periplast component [either sheet-like or polygonal plates (Hill and Wetherbee 1986)]. The genera *Cryptomonas* and *Campylomonas* differ morphologically in the same manner as the haplomorph and diplomorph of *Proteomonas sulcata* (Hill 1991a; Hoef-Emden and Melkonian, in preparation): the *Campylomonas* periplast consists of a continuous sheet, and a long keeled rhizostyle is directed toward the antapex of the cell, whereas in *Cryptomonas* polygonal periplast plates and a shorter nonkeeled rhizostyle are found (Santore 1985; Hill 1991a). Hoef-Emden and Melkonian (in preparation) report dimorphism for several strains of the genus *Cryptomonas,* with the *Campylomonas* phenotype occurring as a second cell type in clonal cultures. The apparently random distribution of phenotypes with periplast sheets or polygonal periplast plates in the SSU rDNA trees most likely reflects the hidden dimorphism in clade CRYP (this study; see Fig. 6). Most strikingly, strain CCAP 979/61 ("*Cryptomonas ovata* var. *palustris*"), an often examined reference strain of the genus *Cryptomonas* (e.g., Gantt et al. 1971; Santore 1985; Hill 1991a), and the authentic strain of *Campylomonas reflexa* (Hill 1991a) differ in their nuclear SSU rDNA in only two nucleotides and in the more variable nucleomorph SSU rDNA in only nine nucleotides (most differences are found in the nonalignable regions), and this is reflected by their very close positioning in both SSU rDNA phylogenies (this study). Moreover, forcing the strains of clade CRYP into two monophyletic sister clades—one clade comprising only strains with sheet-like periplasts, the other clade comprising only strains with polygonal periplast plates—resulted in significantly worse tree topologies for all three alignments of the combined analyses (see Table 3; CRYP sorted).

The distribution of IPC types within the CRYP clade as demonstrated in this study contradicts the recent erection of a new family, the Campylomonadaceae, within this clade, which was based exclusively on IPC and flagellar root characters (Clay et al. 1999), and in fact even renders the genus *Campylomonas* superfluous (Hoef-Emden et al., in preparation).

In the genera *Rhinomonas* and *Storeatula,* two further candidates for a hidden dimorphism were found: the genera share the same biliprotein type (PE 545) and the same type of cell invagination (gullet) but differ in periplast type [periplast sheet vs. distinct plates (Hill and Wetherbee 1988; Hill 1991a)]. Again, the genus with the periplast sheet is reported to have a long keeled rhizostyle [*Storeatula* (Hill 1991a)], whereas the genus with periplast plates displays a short nonkeeled rhizostyle [*Rhinomonas* (Hill 1991a)]. In both trees the SSU rDNA sequences of the two taxa are almost identical. In addition, in clade CHRO at least two types of periplasts are reported for PC 645-bearing taxa; not just the staggered rectangular periplast plates, which are considered typical for the genus *Chroomonas,* are found, but also hexagonal plates [*Komma* (Hill 1991b)]. In strains with PC 630 rectangular staggered plates have been reported (Novarino and Lucas 1993), but also hexagonal plates (Hoef-

Emden, unpublished data) similar to those of *Hemiselmis* and *Komma* (Wetherbee et al. 1986; Hill 1991b). In PROT 3, two genera with different periplast and furrow/gullet types and flagellar root systems cluster closely together [*Hanusia*—periplast sheet-like, furrow, keeled rhizostyle; *Guillardia*—elongated rectangular periplast plates, gullet, nonkeeled rhizostyle (Gillott and Gibbs 1983; Hill and Wetherbee 1990; Deane et al. 1998)].

Signs for a potential dimorphism are thus found throughout the SSU rDNA trees. Probably dimorphism was already present in the ancestor of all cryptophytes. Irrespective of the not yet understood functional significance of dimorphism in the cryptophytes, the taxonomic implications are evident and will affect both the genus and the species concepts of cryptophytes in a profound way.

Conclusions

The comparison of the SSU rDNA phylogenies of the two eukaryotic genomes of the cryptophytes offered interesting insights into the coevolution but also the divergent evolution of the nuclear and nucleomorph rRNA genes. Whereas the composition of the clades in both phylogenies was congruent in most parts of the trees, conspicuous differences were found in evolutionary rates not only within the phylogenetic trees but also between the nuclear and the nucleomorph phylogenies. Different long-branch scenarios have been found: longer branches which were presumably due to an early divergence (*Goniomonas,* nuclear phylogeny), accelerated evolutionary rates of single clades perhaps caused by a genetic bottleneck effect (clade CRYP, nuclear phylogeny), and accelerated evolutionary rates within a clade possibly associated with changes in the mode of nutrition (a subclade within CRYP, nucleomorph phylogeny). The heterogeneous evolutionary rates in the nuclear and nucleomorph data sets resulted in long-branch attraction artifacts when simple evolutionary models were applied. Only excluding the homoplasies by deletion of long-branch taxa including the outgroups improved the resolution of the internal branching order. In these deletion experiments the unrooted nucleomorph SSU rDNA phylogeny could be largely resolved and, thus, provided better resolution than the nuclear SSU rDNA phylogeny. A comparison of the tree topology with the distribution of the phenotypic character pigmentation showed congruence of the clades with the type of biliprotein. In contrast, no congruence could be found between the molecular phylogeny and the type of inner periplast component. Instead, evidence for a hidden cell dimorphism is present throughout the entire cryptophyte diversity.

Acknowledgments. We thank Enrico Guiliani (Cologne) for help with cloning techniques, Joe Felsenstein (Seattle) for helpful advice on bootstrap analysis and Kishino-Hasegawa tests, and Brec Clay (Fort Collins) for supplying us with the *Falcomonas daucoides* strain. We also gratefully appreciate the helpful comments on the manuscript by two anonymous reviewers. This work was funded by the DFG (Deutsche Forschungsgemeinschaft).

References

Apt KE, Collier JL, Grossman AR (1995) Evolution of the phycobiliproteins. J Mol Biol 248:79–96

Arciero DM, Bryant DA, Glazer AN (1988) *In vitro* attachment of bilins to apophycocyanin. II. Determination of the structures of tryptic bilin peptides derived from the phycocyanobilin adduct. J Biol Chem 268:18350–18357

Beale SI, Cornejo J (1991) Biosynthesis of phycobillins. 15,16-Dihydrobiliverdin IXα is a partially reduced intermediate in the formation phycobilins from biliverdin IXα. J Biol Chem 266: 22341–22345

Bhattacharya D, Helmchen T, Bibeau C, Melkonian M (1995) Comparisons of nuclear-encoded small-subunit ribosomal RNAs reveal the evolutionary position of the Glaucocystophyta. Mol Biol Evol 12:415–420

Brett SJ, Perasso L, Wetherbee R (1994) Structure and development of the cryptomonad periplast: a review. Protoplasma 181:106–122

Bruno WJ, Halpern AL (1999) Topological bias and inconsistency of maximum likelihood using wrong models. Mol Biol Evol 16:564–566

Butcher RW (1967) An introductory account of the smaller algae of British coastal waters. Part IV: Cryptophyceae. Fishery Investigations. Ministry of Agriculture, Fisheries & Food, HMSO, London, Ser. IV

Cavalier-Smith T, Couch JA, Thorsteinsen KE, Gilson P, Deane JA, Hill DRA, McFadden GI (1996) Cryptomonad nuclear and nucleomorph 18S rRNA phylogeny. Eur J Phycol 31:315–328

Clay BL, Kugrens P (1999) Characterization of *Hemiselmis amylosa* sp. nov. and phylogenetic placement of the blue-green cryptomonads *H. amylosa* and *Falcomonas daucoides.* Protist 150:297–310

Clay BL, Kugrens P, Lee RE (1999) A revised classification of the Cryptophyta. Bot J Linn Soc 131:131–151

Cornejo J, Beale SI (1997) Phycobilin biosynthetic reactions in extracts of cyanobacteria. Photosynth Res 51:223–230

Deane JA, Hill DRA, Brett SJ, McFadden GI (1998) *Hanusia phi* gen. et sp. nov. (Cryptophyceae): Characterization of '*Cryptomonas* sp. Φ.' Eur J Phycol 33:149–154

Douglas SE, Penny SL (1999) The plastid genome of the cryptophyte alga, *Guillardia theta:* Complete sequence and conserved synteny groups confirm its common ancestry with red algae. J Mol Evol 48:236–244

Douglas SE, Murphy CA, Spencer DF, Gray MW (1991) Cryptomonad algae are evolutionary chimaeras of two phylogenetically distinct unicellular eukaryotes. Nature (London) 350:148–151

Douglas SE, Zauner S, Fraunholz M, Beaton M, Penny S, Deng LT, Wu X, Reith M, Cavalier-Smith T, Maier U-G (2001) The highly reduced genome of an enslaved algal nucleus. Nature (London) 410:1040–1041

Doyle JJ, Doyle JL (1990) Isolation of plant DNA from fresh tissue. Focus 12:13–15

Elwood HJ, Olsen GJ, Sogin ML (1985) The small subunit ribosomal RNA gene from the hypotrichous ciliates *Oxytricha nova* and *Stylonichia pustulata.* Mol Biol Evol 2:399–410

Felsenstein J (1978) Cases in which parsimony or compatibility methods will be positively misleading. Syst Zool 27:401–410

Felsenstein J (1981) Evolutionary trees from DNA sequences: A maximum likelihood approach. J Mol Evol 17:368–376

Felsenstein J (1985) Confidence limits on phylogenies: an approach using the bootstrap. Evolution 39:783–791

Fitch WM (1977) On the problem of discovering the most parsimonious tree. Am Nat 111:223–257

Galtier N, Gouy M, Gautier C (1996) SEAVIEW and PHYLO_WIN: Two graphic tools for sequence alignment and molecular phylogeny. CABIOS 12:543–548

Gantt E, Edwards MR, Provasoli L (1971) Chloroplast structure of the Cryptophyceae. Evidence for phycobiliproteins within the intrathylakoidal spaces. J Cell Biol 48:280–290

Gervais F (1998) Ecology of cryptophytes coexisting near a freshwater chemocline. Freshw Biol 39:61–78

Gillott M, Gibbs SP (1980) The cryptomonad nucleomorph: its ultrastructure and evolutionary significance. J Phycol 16:558–568

Gillott M, Gibbs SP (1983) Comparison of the flagellar rootlets and periplast in two marine cryptomonads. Can J Bot 61:1964–1978

Glazer AN, Wedemayer GJ (1995) Cryptomonad biliproteins—An evolutionary perspective. Photosynth Res 46:93–105

Goldman N (1993) Statistical tests of models of DNA substitution. J Mol Evol 36:182–198

Goldman N, Anderson JP, Rodrigo AG (2000) Likelihood-based tests of topologies in phylogenetics. Syst Biol 49:652–670

Graybeal A (1998) Is it better to add taxa or characters to a difficult phylogenetic problem? Syst Biol 47:9–17

Greenwood AD (1974) The Cryptophyta in relation to phylogeny and photosynthesis. Proc 8th Int Congr Electron Microsc 2:566–567

Guillard RRL, Hargraves PE (1993) *Stichochrysis immobilis* is a diatom, not a chrysophyte. Phycologia 32:234–236

Hendy M, Penny D (1989) A framework for the quantitative study of evolutionary trees. Syst Zool 38:297–309

Hill DRA (1991a) A revised circumscription of *Cryptomonas* (Cryptophyceae) based on examination of Australian strains. Phycologia 30:170–188

Hill DRA (1991b) *Chroomonas* and other blue-green cryptomonads. J Phycol 27:133–145

Hill DRA, Rowan KS (1989) The biliproteins of the Cryptophyceae. Phycologia 28:455–463

Hill DRA, Wetherbee R (1986) *Proteomonas sulcata* gen. et sp. nov. (Cryptophyceae), a cryptomonad with two morphologically distinct and alternating forms. Phycologia 25:521–543

Hill DRA, Wetherbee R (1988) The structure and taxonomy of *Rhinomonas pauca* gen. et sp. nov. (Cryptophyceae). Phycologia 27: 355–365

Hill DRA, Wetherbee R (1989) A reappraisal of the genus *Rhodomonas* (Cryptophyceae). Phycologia 28:143–158

Hill DRA, Wetherbee R (1990) *Guillardia theta* gen. et sp. nov. (Cryptophyceae). Can J Bot 68:1873–1876

Hillis DM, Huelsenbeck JP, Swofford DL (1994) Hobgoblin of phylogenetics? Nature (London) 369:363–364

Huber-Pestalozzi G (1967) Das Phytoplankton des Süβwassers. 3. Teil: Cryptophyceen, Chloromonadinen, Peridineen. In: Thienemann A (ed) Die Binnengewässer. E. Schweizerbart'sche Verlagsbuchhandlung, Stuttgart, Vol 16(3), pp 2–78

Huelsenbeck JP (1995) Performance of phylogenetic methods in simulation. Syst Biol 44:17–48

Hultman T, Bergh S, Moks T, Uhlen M (1991) Bi-directional solid phase sequencing of *in vitro*-amplified plasmid DNA. BioTechniques 10:84–93

Inoue H, Nojima H, Okayama H (1990) High efficiency transformation of *Escherichia coli* with plasmids. Gene 96:23–28

Keeling PJ, Deane JA, Hink-Schauer C, Douglas SE, Maier U-G, McFadden GI (1999) The secondary endosymbiont of the cryptomonad *Guillardia theta* contains alpha-, beta-, and gamma-tubulin genes. Mol Biol Evol 16:1308–1313

Kim J (1996) General inconsistency conditions for maximum parsimony: Effects of branch lengths and increasing numbers of taxa. Syst Biol 45:363–374

Kishino H, Hasegawa M (1989) Evaluation of the maximum likelihood estimate of evolutionary tree topologies from DNA sequence data, and the branching order in Hominoidea. J Mol Evol 29:170–179

Kugrens P, Lee RE, Andersen RA (1986) Cell form and surface patterns in *Chroomonas* and *Cryptomonas* cells (Cryptophyta) as revealed by scanning electron microscopy. J Phycol 22:512–522

Kumar S, Gadagkar SR (2000) Efficiency of the neighbor-joining method in reconstructing deep and shallow evolutionary relationships in large phylogenies. J Mol Evol 51:544–553

Ludwig M, Gibbs P (1989) Localization of phycoerythrin at the lumenal surface of the thylakoid membrane in *Rhodomonas lens.* J Cell Biol 108:875–884

MacColl R, Berns DS, Gibbons O (1976) Characterization of cryptomonad phycoerythrin and phycocyanin. Arch Biochem Biophys 177:265–275

Mahoney MJ (2001) Molecular systematics of *Plethodon* and *Aneides* (Caudata: Plethodontidae: Plethodontini): Phylogenetic analysis of an old and rapid radiation. Mol Phylogenet Evol 18:174–188

Marin B, Klingberg M, Melkonian M (1998) Phylogenetic relationships among the Cryptophyta: analyses of nuclear-encoded SSU rRNA sequences support the monophyly of extant plastid-containing lineages. Protist 149:265–276

McFadden GI, Melkonian M (1986) Use of Hepes buffer for microalgal culture media and fixation for electron microscopy. Phycologia 25:551–557

McFadden GI, Gilson PR, Douglas SE (1994a) The photosynthetic endosymbiont in cryptomonad cells produces both chloroplast and cytoplasmic-type ribosomes. J Cell Sci 107:649–657

McFadden GI, Gilson PR, Hill DRA (1994b) *Goniomonas:* rRNA sequences indicate that this phagotrophic flagellate is a close relative of the host component of cryptomonads. Eur J Phycol 29:29–32

Medlin L, Elwood HJ, Stickel S, Sogin ML (1988) The characterization of enzymatically amplified eukaryotic 16S-like rRNA coding regions. Gene 98:139–151

Meyer SR, Pienaar RN (1984). The microanatomy of *Chroomonas africana* sp. nov. (Cryptophyceae). S Afr J Bot 3:306–319

Mignot J-P (1965) Étude ultrastructurale de *Cyathomonas truncata* From. (Flagellé cryptomonadine). J Microsc (Paris) 4:239–252

Moreira D, Le Guyader H, Philippe H (2000) The origin of red algae and the evolution of chloroplasts. Nature (London) 405:32–33

Morrall S, Greenwood AD (1980) A comparison of the periodic substructures of the trichocysts of the Cryptophyceae and Prasinophyceae. BioSystems 12:71–83

Muse SV (2000) Examining rates and patterns of nucleotide substitution in plants. Plant Mol Biol 42:25–43

Nickrent DL, Starr EM (1994) High rates of nucleotide substitution in nuclear small-subunit (18S) rDNA from holoparasitic flowering plants. J Mol Evol 39:62–70

Novarino G, Lucas IAN (1993) A comparison of some morphological characters in *Chroomonas ligulata* sp. nov. and *C. placoidea* sp. nov. (Cryptophyceae). Nord J Bot 13:583–591

Page RDM (1996) TREEVIEW: An application to display phylogenetic trees on personal computers. CABIOS 12:357–358

Philippe H (2000) Opinion: Long branch attraction and protist phylogeny. Protist 151:307–316

Philippe H, Lopez P, Brinkmann H, Budin K, Germot A, Laurent J, Moreira D, Müller M, Le Guyader H (2000) Early-branching or fast-evolving eukaryotes? An answer based on slowly evolving positions. Proc R Soc Lond B 267:1213–1221

Posada D, Crandall KA (1998) Modeltest: testing the model of DNA substitution. Bioinformatics 14:817–818

Roberts KR, Stewart KD, Mattox KR (1981) The flagellar apparatus of *Chilomonas paramecium* (Cryptophyceae) and its comparison with certain zooflagellates. J Phycol 17:159–167

Rodríguez R, Oliver JF, Marín A, Medina JR (1990) The general stochastic model of nucleotide substitution. J Theor Biol 142:485–501

Saiki RK, Gelfand DH, Stoffel S, Scharf SJ, Higuchi R, Horn GT, Mullis KB, Erlich HA (1988) Primer-directed enzymatic amplification of DNA with a thermostable DNA polymerase. Science 293: 487–491

Saitou N, Nei M (1987) The neighbor-joining method: A new method for reconstructing phylogenetic trees. Mol Biol Evol 4:406–425

Sambrook J, Fritsch EF, Maniatis T (1989) Molecular cloning: A laboratory manual, 2nd ed. Cold Spring Harbor Laboratory Press, Cold Spring Harbor, NY

Santore UJ (1985) A cytological survey of the genus *Cryptomonas* (Cryptophyceae) with comments on its taxonomy. Arch Protistenkd 130:1–52

Sepsenwol S (1973) Leucoplast of the cryptomonad *Chilomonas paramecium.* Exp Cell Res 76:395–409

Sitte P (1993) Symbiogenetic evolution of complex cells and complex plastids. Eur J Prot 29:131–143

Starr RC, Zeikus JA (1993) UTEX—The Culture Collection of Algae at the University of Texas at Austin. J Phycol 29 (Suppl):1–106

Surek B, Beemelmanns U, Melkonian M, Bhattacharya D (1994) Ribosomal RNA sequence comparison demonstrate an evolutionary relationship between Zygnematales and charophytes. Plant Syst Evol 191:171–181

Swofford DL (1998) PAUP*. Phylogenetic analysis using parsimony (* and other methods), version 4. Sinauer Associates, Sunderland, MA

Tamura K, Nei M (1993) Estimation of the number of nucleotide substitutions in the control region of mitochondrial DNA in humans and chimpanzees. Mol Biol Evol 10:512–526

Van de Peer Y, Baldauf SL, Doolittle WF, Meyer A (2000) An updated and comprehensive rRNA phylogeny of (crown) eukaryotes based on rate-calibrated evolutionary distances. J Mol Evol 51:565–576

Wedemayer GJ, Kidd DG, Wemmer DE, Glazer AN (1992) Phycobilins of cryptophycean algae. Occurrence of dihydrobiliverdin and mesobiliverdin in cryptomonad biliproteins. J Biol Chem 267: 7315–7331

Wemmer DE, Wedemayer GJ, Glazer AN (1993) Phycobilins of cryptophycean algae. Novel linkage of dihydrobiliverdin in a phycoerythrin 555 and a phycocyanin 645. J Biol Chem 268:1658–1669

Wetherbee R, Hill DRA, McFadden GI (1986) Periplast structure of the cryptomonad flagellate *Hemiselmis brunnescens.* Protoplasma 131: 11–22

Wu C-I, Li W-H (1985) Evidence for higher rates of nucleotide substitution in rodents than in man. Proc Natl Acad Sci USA 82:1741–1745

Yang Z (1996) Among-site variation and its impact on phylogenetic analyses. Trends Ecol Evol 11:367–372

Zhao K-H, Deng M-G, Zheng M, Zhou M, Parbel A, Storf M, Meyer M, Strohmann B, Scheer H (2000) Novel activity of a phycobiliprotein lyase: Both the attachment of phycocyanobilin and the isomerization to phycoviolobilin are catalyzed by the proteins PecE and PecF encoded by the phycoerythrocyanin operon. FEBS Lett 469:9–13